



ELSEVIER

Available online at www.sciencedirect.com

SCIENCE @ DIRECT®

Proceedings of the Combustion Institute 30 (2004) 415–421

Proceedings
of the
Combustion
Institute

www.elsevier.com/locate/proci

Nonpremixed ignition of H₂/air in a mixing layer with a vortex

X.L. Zheng, J. Yuan, C.K. Law*

Department of Mechanical and Aerospace Engineering, Princeton University, Princeton, NJ 08540, USA

Abstract

The ignition of a laminar non-premixed H₂/air mixing layer with an embedded vortex was computationally studied with detailed chemistry and transport. The initial vortex velocity and pressure fields were specified based on the stream function of an incompressible nonviscous vortex. The fuel side is pure hydrogen at 300 K, and the oxidizer side is air at 2000 K. The vortex evolution process was found to consist of two ignition events. The first ignition occurs in a diffusion mode with chain branching reactions dominating. The second ignition takes place in the premixed mode, with more chemical reactions involved, and is significantly affected by the heat and species generated in the first ignition event. The coupling between the most reactive mixture fraction and scalar dissipation rate was verified to be crucial to the ignition delay. The effects of the vortex strength, characteristic size, and its center location were individually investigated. For all vortex cases, the ignition delay was shorter than that of the 1D case. Furthermore, the ignition delay has a nonmonotonic dependence on all the vortex parameters.

© 2004 The Combustion Institute. Published by Elsevier Inc. All rights reserved.

Keywords: Vortex; Ignition; Hydrogen combustion

1. Introduction

Recently, there has been considerable interest in understanding the coupled influence of fluid dynamics and chemistry on ignition in well-defined flow fields. Since the oxidation chemistry of hydrogen is simple and yet embodies the essential features of chain mechanisms, it has been extensively used in such studies. Specifically, numerical and experimental studies on the forced ignition of hydrogen by heated air in laminar counterflows [1–8] showed the preservation of the characteristic Z-shaped pressure–temperature homogeneous ignition boundary, while experimental [9,10] and numerical [11–14] studies on

ignition in turbulent flows showed a decrease in ignition delay times as compared to laminar ignition. Furthermore, the experiments also indicated the existence of optimal turbulent intensities and scales for ignition.

A rational interpretation of the above results on turbulent ignition, however, has been hindered by the complexity of flow. Consequently, ignition has been studied in an elemental structure of turbulent flows, the vortex, but with less accurate descriptions of other aspects of the problem. For example, Macareg et al. [15] studied vortex ignition with equal oxidizer and fuel temperatures using asymptotic analysis. Thévenin and Candel [16] performed numerical simulation of vortex ignition, assuming constant density and unity Lewis number, and with one-step reaction. It is reasonable to expect that the simplified chemistry and decoupled flow field descriptions in these

* Corresponding author. Fax: +1 609 258 6233.
E-mail address: cclaw@princeton.edu (C.K. Law).

studies could have overlooked some aspects of the couplings between fluid mechanics and chemical kinetics in turbulent ignition.

In view of the above considerations, the goal of the present study was to examine the fully coupled effects of chemistry and fluid mechanics on ignition, using higher-order numerical simulation with detailed chemistry and transport. The particular problem studied was ignition in a mixing layer embedded in a vortex. The variation of the flow field was achieved by varying the vortex characteristics: the vortex strength, the length scale of the vortex, and its position relative to the mixing layer.

In the following, the numerical methodology and the initial conditions are discussed first. This will be followed by examining the evolution history of the mixing layer in a vortex and by comparing it to the one-dimension (1D) pure mixing layer case. Finally, the effects of different vortex characteristics will be investigated.

2. Numerical methodology and initial conditions

The nonpremixed ignition in a mixing layer of cold hydrogen and hot air, with and without a single vortex in the domain, was investigated. The schematic of the problem configuration is illustrated in Fig. 1. The fuel side is pure hydrogen at 300 K, and the oxidize side is hot air at 2000 K. Calculations were performed with the code developed by Yuan et al. [17], in which the full compressible Navier–Stokes, species, and energy equations were solved with a sixth-order central difference scheme [18,19] and a third-order Runge–Kutta scheme. To incorporate the effects of detailed chemistry and transport, the CHEM-KIN package is integrated to the code [20,21]. The Runge–Kutta integration scheme essentially

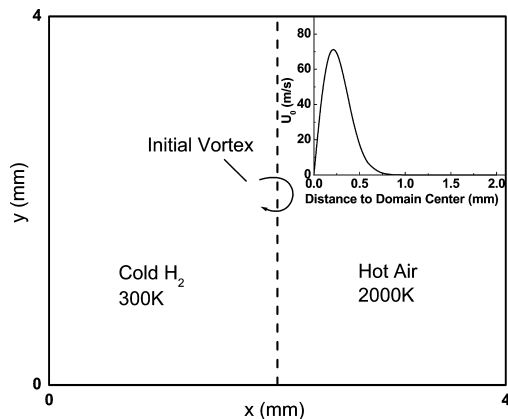


Fig. 1. Schematic of the problem configuration. The inset is the initial velocity distribution along the radial direction of the vortex.

ensures full coupling between fluid dynamics and chemical reactions. The chemical reaction mechanism chosen was that of Mueller et al. [22], involving 9 species and 21 reversible reactions. For the vortex-free, 1D calculation, a regular grid with 251 points was employed for the 4 mm domain, which had a resolution of 16 μm . The computation domain for the vortex case was a 4 mm \times 4 mm, with a uniform grid of 251 \times 251. The adoption of such a fine grid was to ensure that all species profiles were fully resolved. Pressure was calculated from the inner domain using the conservation equations. Non-reflective boundary condition [17] was applied to all of the four boundaries.

Computation was initiated with a uniform profile on both sides of the domain. The jumps in the temperature and species concentrations across the mixing layer were smoothed by a hyperbolic-tangent profile with a constant stiffness parameter for all computations [13]. The specific value of the stiffness parameter was chosen such that there were at least 10 grid points to describe the transition. The mean flow was quiescent at time zero, and the velocity field of the vortex was defined by the stream function for an incompressible non-viscous vortex [19]:

$$\varphi = C \exp\left(-\frac{x^2 + y^2}{2R_c^2}\right),$$

$$\begin{pmatrix} u \\ v \end{pmatrix} = \begin{pmatrix} \frac{\partial \varphi}{\partial y} \\ -\frac{\partial \varphi}{\partial x} \end{pmatrix} = \frac{C}{R_c^2} \exp\left(-\frac{x^2 + y^2}{2R_c^2}\right) \begin{pmatrix} -y \\ x \end{pmatrix}, \quad (1)$$

where C represents the vortex strength and R_c is the characteristic vortex radius. The vortex center coincides with that of the domain unless indicated otherwise. In the inset of Fig. 1, the initial circumferential velocity is plotted along the radial direction of the vortex, which shows that the vortex effect is concentrated over a certain range.

3. Results and discussion

3.1. Dynamics of evolution

A typical evolution history of the mixing layer is shown in Fig. 2, where the overall heat release rates at three different times are plotted across the unperturbed mixing layer, through the center of the vortex, for the 1D and vortex cases; the 1D case is studied as a quantitative reference to identify the effects of vortex on ignition. Thus for the 1D case, Fig. 2A shows that, after ignition is initiated at time LI (L, laminar; I, ignition), a diffusion flame is established at time LD (D, diffusion flame). This flame subsequently becomes weakened due to the consumption of the reac-

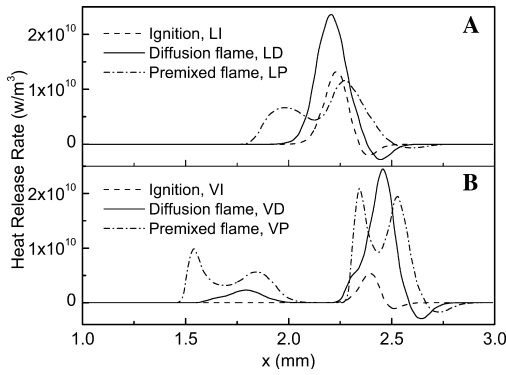


Fig. 2. Distribution of the heat release rate along the domain center line in the x -direction at representative stages of evolution: (A) 1D case, (B) vortex case.

tants, and a pair of premixed flames originates from the ignition point, propagating to each side of the mixing layer, as shown by the profile at time LP (P, premixed flame). This result is similar to those from previous theoretical work [23] and numerical simulation [13,24]. The ignition dynamics for the vortex case is similar to that of the 1D case, as shown in Fig. 2B, with V, vortex. The additional reaction zone on the left side of the domain (Fig. 2B) is the tip of the deformed mixing layer induced by the vortex rollup, and as such its evolution dynamics is similar to that of the primary ignition zone.

To gain an overview of the evolution process, the maximum heat release rate, q_{max} , within the computation domain is plotted in Fig. 3 as a function of time for both the vortex and 1D cases. It is seen that, compared to the 1D case, the vortex case has higher heat release rates and an additional peak. We shall indicate these two peaks as the occurrence of the first and second ignition events. The corresponding ignition delay time

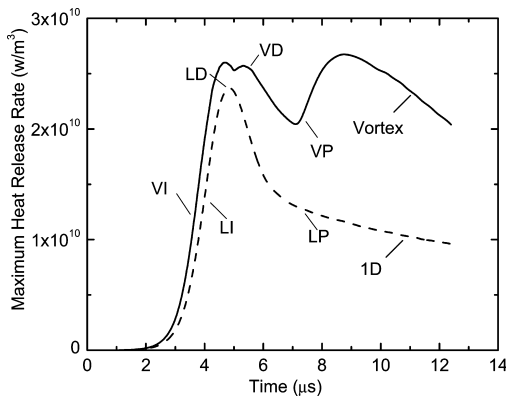


Fig. 3. Time-dependent evolution history of the maximum heat release rate for the 1D and vortex ignition.

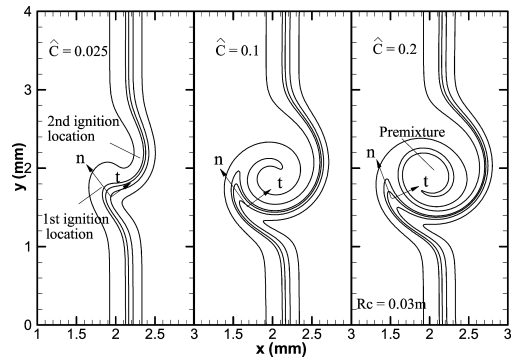


Fig. 4. The iso-level contours of mixture fraction at the first ignition for three different vortex strengths.

can be defined as the inflection point of the heat release profile, $\partial^2 q_{max} / \partial t^2 = 0$. The two ignition locations are indicated only in Fig. 4 because they are similar for all three cases.

To interpret the above behavior, we first define the mixture fraction Z , which characterizes the extent of mixing between fuel and oxidizer, and the scalar dissipation rate χ :

$$Z = \frac{(1/2)Z_H/W_H + (Z_{O,0} - Z_O)/W_O}{(1/2)Z_{H,0}/W_H + Z_{O,0}/W_O}, \quad (2)$$

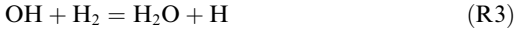
$$\chi_{D_i} = 2D_i|\nabla Z|^2, \quad \chi_T = 2\frac{\lambda}{\rho c_p}|\nabla Z|^2, \quad (3)$$

where Z_H and Z_O are the elemental mass fractions of H and O, and the subscript 0 represents the initial conditions on the oxidizer and fuel sides, respectively [13]. The mixture fraction is 1 on the fuel side, 0 on the air side, and 0.028 for the stoichiometric situation of our initial configuration. Furthermore, D_i is the local diffusion coefficient of the i th species relative to the mixture, λ the mixture averaged heat conduction coefficient, ρ is the mixture density and c_p is the specific heat constant.

As the vortex rolls up in the mixing layer, the Z contours deform, as shown in Fig. 4, and are broadened near the vortex center in the normal direction of the reaction zone. Consequently, the normal gradient of Z , as well as χ , is reduced. Recognizing that [25] the reduced Damköhler number is inversely proportional to the scalar dissipation rate, i.e., $Da \sim 1/D|\nabla Z|^2$, a smaller χ will lead to an earlier ignition, and vice versa. As a result, vortex ignition ($3.8 \mu s$) occurs earlier than the 1D case ($4.1 \mu s$) due to the reduced scalar dissipation rate (Fig. 3). Moreover, the local scalar dissipation rate characterizes the local heat loss caused by convection and diffusion [11,25], so a reduced χ corresponds to less heat loss, and therefore higher reactivity, for the vortex case, as shown in Fig. 3.

3.2. Chemical structure

As the vortex rolls up and redistributes the reactant and temperature fields, the associated chemical reactions are expected to vary. For both the vortex and 1D cases, the first ignition event is found to be mainly controlled by the three high-temperature chain branching reactions:



The ignition chemistry and dynamics are different for the second ignition event because radicals generated by the first ignition are now available, and the deformation of the mixing layer is more severe because of the longer delay time.

Figure 5 plots for the 1D case the total heat release rate as well as the individual reaction heat release rates for the premixed flames at time LP. It is seen that although the total heat release rate has only two peaks corresponding to the two premixed flames, the distribution of the individual heat release rates has a three-zone structure, with different chemical reactions taking place in each zone. Specifically, the rightmost zone is under very high temperatures, around 2100 K. Consequently, the major reactions are those of chain branching, R1–R3, and water formation:



The leftmost reaction zone is at temperatures below 900 K, so only the exothermic reactions:



are active. The middle zone is at intermediate temperatures, and hence consists of both the chain

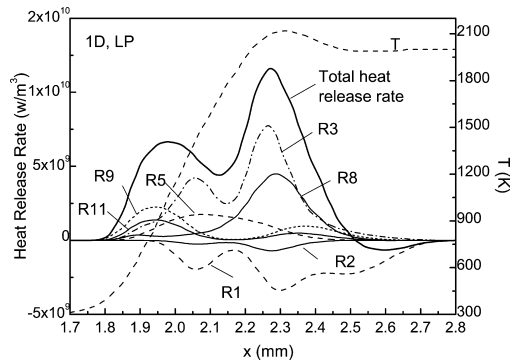


Fig. 5. Profiles for the total heat release rate, the heat release rates by individual reactions, and temperature at time LP along the domain center line in the x -direction, for the 1D case.

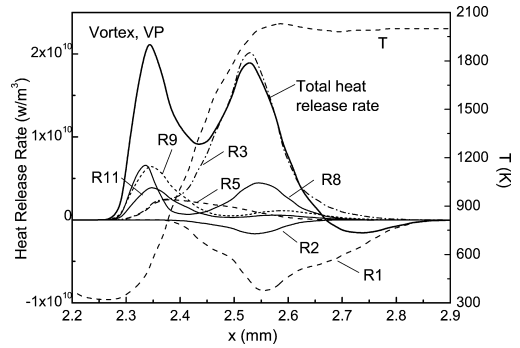


Fig. 6. Profiles for the overall heat release rate, the heat release rates by individual reactions, and temperature at time VP along the domain center line in the x -direction, for the vortex case.

branching reactions R1 and R3, and the recombination reaction

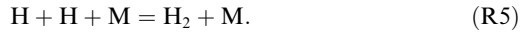


Figure 6 shows the corresponding situation for the vortex case, at time VP. Compared to Fig. 5, it is seen that the same group of reactions contributes to the heat release for both cases. However, the vortex case has only two reaction zones, which correspond to the rightmost and leftmost reaction zones of Fig. 5. The middle reaction zone of the 1D case is absorbed into the surrounding layers for the vortex case. This is due to the fact that the mixing layer is deformed and compressed by the rollover motion of the vortex. Moreover, the compression of the mixing layer increases the temperature and reactant concentration gradients across the flames. Consequently, more fuel is fed to the reaction zone for the vortex case. Furthermore, since the heat release rate is an extensive quantity, the faster flow rate associated with the stronger gradient also leads to increased fuel supply to the ignition kernel. Consequently, the vortex case has a higher heat release rate.

3.3. Ignition location in the vortex case

One important finding from previous numerical simulations of autoignition in turbulent flows [11] is that autoignition in nonhomogeneous mixtures is located where the mixture fraction Z assumes its most reactive value, Z_{MR} , and the corresponding scalar dissipation rate χ_{MR} is low. The quantity Z_{MR} is determined by the corresponding 1D calculation, and the value is chosen at the peak heat release rate location when ignition occurs. For the present study, Z_{MR} equals 0.04 when the initial oxidizer temperature is 2000 K, and the reaction zone near Z_{MR} can be referred to as the ignition kernel. To verify the above criterion, χ_{MR} , the heat release rate and

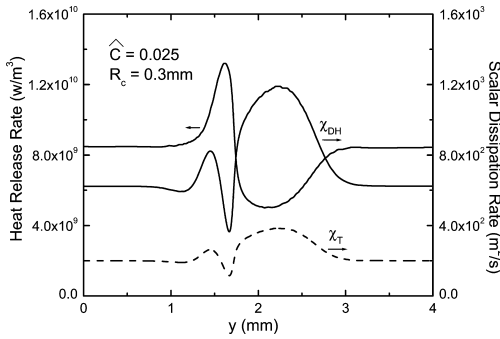


Fig. 7. Distribution of the heat release rate and scalar dissipation rates along the Z_{MR} contour at the first ignition for $\hat{C} = 0.025$ and $R_c = 0.03$ m.

the scalar dissipation rate are plotted along the iso-value $Z_{MR} = 0.04$ contour at the first ignition event for the vortex case in Fig. 7. It is seen that $\chi_{DH} = 2D_H|\nabla Z|^2$ shares a similar trend with $\chi_T = 2\lambda/\rho c_p|\nabla Z|^2$, as well as the scalar dissipation rates of all other species, which are not shown. It illustrates that preferential diffusion and non-unity Lewis number do not affect the trend of χ . This was not clear in previous studies because either unity Lewis number was assumed [25] or the influence of the diffusion coefficient was neglected [16]. Hence, the criterion χ_{MR} is able to locate the ignition spots in nonhomogeneous situations, even with detailed chemistry and transport.

3.4. Effect of vortex characteristics

The above results show that ignition is strongly affected by the vortex motion through the scalar dissipation rate. We now study how ignition is affected by the vortex motion, which is characterized by three parameters, the vortex strength C , the vortex radius R_c (Eq. (1)), and the initial location of the vortex in the mixing layer.

3.4.1. Influence of vortex strength

In Fig. 8, the ignition delay times for the first and second ignition events are plotted as a function of the nondimensional vortex strength, defined as $\hat{C} = C/(a_0L_0)$, where a_0 is the speed of sound, 500 m/s, and L_0 is the domain size, 4 mm. It is seen that the first ignition occurs earlier for the vortex case, and that both ignition delays depend on the vortex strength in a similar manner. This is due to the fact that since the heat and radical sources for the second ignition are primarily supplied by the products formed by the first ignition, the second ignition is directly controlled by the first ignition event. Figure 8 shows further that the ignition delay varies nonmonotonically with the vortex strength. This behavior is closely related to

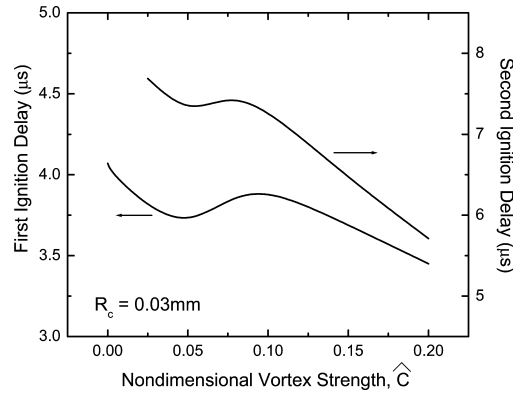


Fig. 8. First and second ignition delays as function of the nondimensional vortex strength.

the variation of the scalar dissipation rate χ along the Z_{MR} contour. Specifically, the scalar dissipation rate is composed of the normal (n) and tangential (t) components of the mixture fraction gradients in the reaction zone, as shown in Fig. 4. For the 1D case, the contribution to χ solely comes from the normal component of the gradient. For the vortex case, when its strength is weak and the rollup speed is small, the reaction contour is only slightly wrinkled, as shown in Fig. 4 for $\hat{C} = 0.025$. Consequently, the normal gradient of Z in the tip region is reduced during roll-up, while there is a small increase in the tangential component leading to a net reduction in χ_{MR} and hence the ignition delay. With an increase in the vortex strength to $\hat{C} = 0.1$, the tangential dimension of the reaction zone is reduced, leading to an increase in the tangential gradient, and hence the ignition delay. Finally, when the vortex becomes even stronger, to $\hat{C} = 0.2$, a sizable pocket of the unburned mixture is formed. This premixture is hotter than the cold hydrogen, and therefore reduces the heat loss from the ignition region to the surrounding by reducing the temperature gradient, leading to early ignition.

3.4.2. Influence of vortex size

The typical integral scale in the turbulent ignition experiments of [10] was about 2–3 mm. However, since the domain of the present study was 4 mm, we have limited the region of influence by the vortex, defined as four times R_c , to be about 1–2 mm.

To isolate the effects of the vortex size, the nondimensional vortex strength is fixed at 0.025, which lies in the region where the normal gradient of Z is much larger than that of the tangential one, and the premixture pocket size does not have enough time to develop. In Fig. 9, the vortex ignition delay, normalized by the 1D value, is plotted against the vortex radius R_c , and it shows that

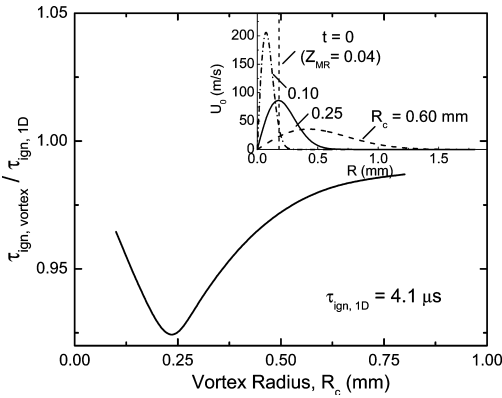


Fig. 9. Nondimensional ignition delay as function of the characteristic vortex size. The inset is the initial velocity distribution along the vortex radial direction for different vortex characteristic sizes.

there exists an optimal vortex radius for minimum ignition delay. The initial velocity distributions for different R_c 's are plotted as a function of distance from the vortex center in the inset of Fig. 9. The dashed straight line represents the initial contour of Z_{MR} , at 0.04. The circumferential velocity experienced by this contour determines the deformation of the ignition kernel, which leads to a modification of χ_{MR} , and hence the ignition delay. With increasing vortex radius R_c , the maximum velocity in the domain decreases according to Eq. (1). At the same time, the location of the peak velocity shifts further away from the center. Once the ignition kernel encounters the maximum possible circumferential velocity, it is substantially elongated. This reduces χ_{MR} , and consequently leads to a minimum value for the ignition delay. The existence of an optimal vortex radius for minimum ignition delay can be anticipated by recognizing the fact that the ignition delay is expected to approach the 1D value, as R_c approaches zero and infinity; in the latter case, the entire computational domain is a tiny spot in the center of the vortex and experiences no rollup.

3.4.3. Influence of vortex location

To study the effects of vortex location, we again fix the nondimensional vortex strength at 0.025 and the vortex radius at 0.3 mm. The vortex center is moved in the direction normal to the mixing layer. Figure 10 shows that the ignition delay exhibits a W-shaped dependence on the displacement distance, which is positive and negative when the vortex center is located in the air and the hydrogen sides, respectively. The (absolute) values of the initial velocity distribution along the x -axis are shown in the inset of Fig. 10. Mechanistically, as the vortex traverses across the mixing layer, the circumferential velocity experienced by the ignition kernel varies correspond-

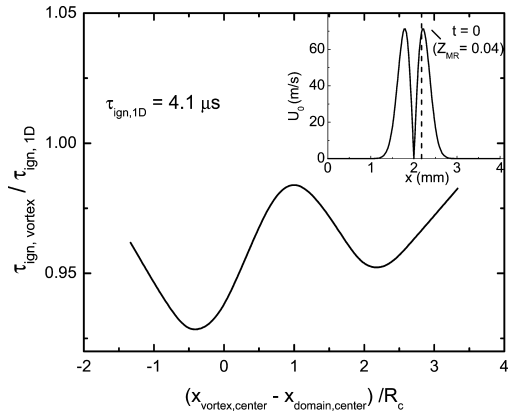


Fig. 10. Nondimensional ignition delay time as function of the nondimensional distance between the vortex center and the domain center. The inset is the absolute value of the initial velocity distribution on both sides of the vortex.

ingly. Consequently, as the local velocity fluctuates from high to low values, ignition is correspondingly facilitated and retarded.

4. Concluding remarks

The ignition of nonpremixed hydrogen/air in a laminar mixing layer with an embedded vortex was numerically studied with detailed chemistry and transport. The vortex evolution process was found to consist of two ignition events. The first ignition occurs in a diffusion mode with chain branching reactions dominating, and the delay time is always shorter than that of the 1D case. The second ignition takes place in a premixed mode with more chemical reactions involved, for which the reactants and species gradients across the mixing layer are increased due to the vortex rollup. This causes more fuel to be fed to the reaction zone, and consequently the heat release rate is significantly higher than that of the 1D case.

Ignition delay was found to be closely controlled by the scalar dissipation rate on the most reactive mixture fraction contour, which is composed of the normal and tangential components of the mixture fraction gradients at the reaction zone. The coupling between the reduction of the normal gradient and increase of the tangential gradient leads to a nonmonotonic dependence of the first ignition delay on the vortex strength. Moreover, for higher vortex strengths, a sizable pocket of the unburned mixture is formed before ignition. This pocket is at a higher temperature than the cold fuel, and therefore reduces the heat loss from the ignition kernel to the surrounding and facilitates ignition. Since the second ignition is facilitated by the heat release and radical pools

generated by the first ignition, it has a similar dependence on vortex strength as the first one.

There exists an optimal vortex size for ignition, for which the rollup velocity experienced by the most reactive mixture fraction contour achieves the possible maximum value and the scalar dissipation rate is the lowest. Similarly, the ignition delay exhibits a W-shaped dependence on the displacement distance of the vortex center, as a consequence of the variation of the rollup velocity.

Acknowledgment

This work was supported by the Army Research Office under the technical monitoring of Dr. David Mann.

References

- [1] N. Darabiha, S. Candel, *Combust. Sci. Technol.* 86 (1–6) (1992) 67–85.
- [2] T.G. Kreutz, M. Nishioka, C.K. Law, *Combust. Flame* 99 (3–4) (1994) 758–766.
- [3] G. Balakrishnan, M.D. Smooke, F.A. Williams, *Combust. Flame* 102 (3) (1995) 329–340.
- [4] C.G. Fotache, T.G. Kreutz, D.L. Zhu, C.K. Law, *Combust. Sci. Technol.* 109 (1–6) (1995) 373–393.
- [5] T.G. Kreutz, C.K. Law, *Combust. Flame* 104 (1–2) (1996) 157–175.
- [6] T.G. Kreutz, C.K. Law, *Combust. Flame* 114 (3–4) (1998) 436–456.
- [7] C.G. Fotache, C.J. Sung, C.J. Sun, C.K. Law, *Combust. Flame* 112 (3) (1998) 457–471.
- [8] C.J. Sung, C.K. Law, *Combust. Sci. Technol.* 129 (1–6) (1997) 347–360.
- [9] J.D. Blouch, C.J. Sung, C.G. Fotache, C.K. Law, *Proc. Combust. Inst.* 27 (1998) 1221–1228.
- [10] J.D. Blouch, C.K. Law, *Combust. Flame* 132 (3) (2003) 512–522.
- [11] E. Mastorakos, T.A. Baritaud, *Combust. Flame* 109 (1–2) (1997) 198–223.
- [12] H.G. Im, J.H. Chen, C.K. Law, *Proc. Combust. Inst.* 27 (1998) 1047–1056.
- [13] R. Hilbert, D. Thévenin, *Combust. Flame* 128 (1–2) (2002) 22–37.
- [14] T. Echekki, J.H. Chen, *Combust. Flame* 134 (3) (2003) 169–191.
- [15] M.G. Macaraeg, T.L. Jackson, M.Y. Hussaini, *Combust. Sci. Technol.* 87 (1–6) (1992) 363–387.
- [16] D. Thévenin, S. Candel, *Phys. Fluids* 7 (2) (1995) 434–445.
- [17] J. Yuan, Y. Ju, C.K. Law, *Proceedings of the 3rd Joint Meeting of the US Sections of Combustion Institute* 27, Chicago, 2003, pp. 1221–1228.
- [18] T. Poinsot, S.K. Lele, *J. Compt. Phys.* 101 (1992) 104–129.
- [19] T. Poinsot, S.K. Lele, *J. Compt. Phys.* 103 (1992) 16–42.
- [20] R.J. Kee, F.M. Rupley, J.A. Miller, Report No. SAND 89-8009B, Sandia National Laboratories, 1989.
- [21] R.J. Kee, J. Warnatz, J.A. Miller, Report No. SAND 83-8209, Sandia National Laboratories, 1983.
- [22] M.A. Mueller, T.J. Kim, R.A. Yetter, F.L. Dryer, *Int. J. Chem. Kinet.* 31 (1999) 113–125.
- [23] A. Liñán, A. Crespo, *Combust. Sci. Technol.* 14 (1–3) (1976) 95–117.
- [24] D. Thévenin, S. Candel, *Combust. Sci. Technol.* 91 (1–3) (1993) 73–94.
- [25] W.T. Ashurst, F.A. Williams, *Proc. Combust. Inst.* 23 (1990) 543–550.

Comment

Sebastien Candel, EM2C Lab, CNRS, Ecole Centrale Paris, France. Some years ago [1] we examined this problem using the thermo diffuse approximation and we found that there were two regimes of ignition depending on the temperature of the hot stream and on the vortex strength. In one case ignition was occurring in the premixed core formed near the vortex center. In the other, it took place in the braids in the form of a diffusion flame associated with two premixed flames. Did you vary your hot stream temperature and did you observe such effects?

Reference

- [1] Candel, et al., *Phys. Fluids* (1996).

Reply. Due to limitations of the computation domain and time, we only studied situations where the hot stream temperature is high, at 2000 K. The results showed that ignition is first initiated around the core region, in agreement with the high-temperature ignition regime (Ref. [1] in paper). Since we did not study situations involving lower values of the hot stream temperature, we are not prepared to comment on the possible responses.